archives
of thermodynamics
Vol. **41**(2020), No. 4, 269–283
DOI: 10.24425/ather.2020.135988

Simulation and numerical analysis of a rectangular pipe with transversal baffle – comparison between zigzag and plane baffles

CHAFIKA ZIDANI*
BOUMEDIENNE BENYOUCEF
FAOUZI DIDI
NABILA GUENDOUZ

Unit of Research on Materials and Renewable Energies – URMER – Department of Physics, Faculty of Sciences, Abou Bekr Belkaïd University, BP 119–13000 – Tlemcen, Algeria

Abstract The airflow through a two-dimensional horizontal rectangular cross-section channel in the presence of two baffles has been numerically examined and analyzed in the steady turbulent regime. The baffles were of the zig-zag type or plane one. The calculations are based on the finite volume approach and the average Navier–Stokes equations along with the energy equation, have been solved using the SIMPLE algorithm. The non-uniform structured quadrilateral-type element mesh is used in this study. The fluid flow patterns represented for Reynolds numbers based on the hydraulic diameter of the channel ranging from 5000 to 20 000. Effects of various Reynolds number values on flow fields, dimensionless axial velocity profiles, as well as local and average friction coefficients in the test channel is presented. The obtained results show that the flow structure is characterized by strong deformations and large recirculation regions. In general, the fluid velocity and skin friction loss rise with the increase in the flow rate and hence the Reynolds number.

Keywords: Dynamic simulation; Turbulent flow; Forced convection; Rectangular pipe; Baffle

*Corresponding Author. Email: zidanichafika10@gmail.com

Nomenclature

C_f	–	friction coefficient
C_{f0}	–	friction coefficient without baffles
Cp	–	specific heat at constant pressure, J/kg·K
D	–	distance between two baffles, m
D_h	–	hydraulic diameter of channel, m
D_ω	–	cross diffusion term, m^2/s
e	–	fin height, m
G_k	–	production of turbulent kinetic energy due to velocity gradient, m^2/s^2
G_ω	–	production of kinetic energy due to buoyancy, m^2/s^2
h	–	baffle height, m
H	–	channel height, m
k	–	turbulent kinetic energy, m^2/s^2
L	–	channel length, m
L_1	–	distance upstream of the first baffle, m
L_2	–	distance downstream of the second baffle, m
P	–	pressure, Pa
Re	–	Reynolds number
P	–	pressure, Pa
Pr	–	Prandtl number
T	–	temperature, K
T_{in}	–	inlet temperature, K
T_W	–	temperature of the lower and upper walls, °C
C_{pf}	–	specific heat of fluid, J/kg·K
C_{ps}	–	specific heat of solid, J/kg·K
S_k, S_ω	–	source term for k and ω
u_i	–	components of velocity in direction x_i, m/s
u_j	–	components of velocity in direction x_j, m/s
U_{in}	–	inlet velocity m/s,
U	–	average speed through the section, m/s
$\overline{U}$	–	average speed inside the channel, m/s
u, v	–	velocity of fluid in y, x directions, m/s
$\bar{\nu}$	–	velocity vector, m/s
x_i, x_j	–	Cartesian coordinates, m
Y_k, Y_x	–	dissipation of k and ω, m^2/s

Greek symbols

ω	–	dissipation rate of specific turbulence energy, m^2/s
ρ	–	air density, kg/m^3
μ_f	–	dynamic viscosity of fluid, kg/m·s
μ_e	–	effective viscosity, Pa s
ν	–	kinematic viscosity, $kg/(s^2m)$
δ	–	fin width, m
ΔP	–	pressure losses
ε	–	turbulent dissipation energy, m^2/s^2
ρ_f	–	density of air, kg/m^3
ρ_s	–	density of solid, kg/m^3

δ – fin width, m
λ – thermal conductivity, W/m K
σ_k, σ_ε, σ_t – constant value for the standard turbulence model of k-ω
τ_w – shear stress at the wall, Pa

Subscripts

in – inlet of the channel section
out – outlet of the channel section
t – turbulent
w – walls
f – fluid
s – solid

1 Introduction

The main objective of the work is to show the possibility of increasing heat transfer rates using baffles. Presented is a bibliographical study on the various works published in the subject. At the passage around the chicane, the flow separates. When there is a flow separation, the flatting region is a local maximum region of heat transfer; whereas on the other hand, that of separation is a region of the local minimum. The major drawback of this method is the increase in the pressure drop and the downstream establishment of baffles or hot pockets obstacles, caused by the low speeds of the secondary vortex. The nature and intensity of the disturbance around the baffles, which are the main parameters of the increase in heat transfer, strongly depend on their geometrical characteristics. There is a great deal of works involved in the flow studies around baffles, both of experimental and numerical background. Several researchers have carried out work on different types of baffles. Numerical studies carried out examined the heat transfer of a periodic laminar flow in a rectangular channel provided with formally placed V-shaped baffles, symmetrical on the upper walls, and lower. Promvonge and Kwankaomeng [1] and Abene *et al.* [2] studied a solar collector using different obstacles. The application is made for the drying of grapes. They found that introducing barriers into the air channel is a very important factor in improving the sensor performance. They also showed that the dimensions, shape and orientation of these obstacles have a significant impact on the efficiency of the solar collector. Sripattanapipat and Promvonge [3] propose in their study baffles in form of diamonds. They characterized the heat transfer rate by the distribution of the Nusselt number as a function of the wall length and Reynolds number. The work is done for several diamond angles (50° to 350°). They concluded that the

flat baffle ensures an optimal heat transfer rate. The latter is characterized by the distribution of the Nusselt number, against the baffle oriented at an angle of 350° and gives a poor heat transfer rate. Researchers have proposed to increase the heat transfer between the absorber and the coolant in a planar solar sensor by adding obstacles. In the case of obstacles fixed on the insulation, the choice of geometric shapes of obstacles used must satisfy certain criteria. Indeed the shape and the arrangement of the obstacles affect the flow of air during its trajectory. Obstacles ensure good absorption of the absorber, create turbulence and reduce inactive areas in the collector [4]. In order to improve the performance of flat-air solar collectors, the sensor's dynamic airflow has been etched with artificial roughness of different shapes and arrangements to optimize thermal performance Aoues *et al.* [5].

Among the experimental studies, we mention the work of Yuan *et al.* [6]. They studied experimentally a case of duct with periodic rectangular fins along the direction of the channel. A comparative study was conducted on four models with fins derived. They showed an increase in heat transfer by comparison with that obtained for a smooth duct. The dynamic and thermal behavior of turbulent and transient flows in pipes in the presence of obstacles and ribs has also been studied experimentally and numerically by Acharya *et al.* [7]. The k-ε turbulence model is used in their numerical simulation. Wilfried has experimentally studied the influence of the inter-baffle distance and the distance between the baffle and the shell on the thermal performance of a tubular heat exchanger [8]. In order to evaluate heat transfer and pressure drop in a rectangular pipe with overlapped baffles, Molki *et al.* [9] conducted an experimental study. The study found that baffles increase pressure drop much quicker and also increase the heat transfer coefficient.

We study two different geometries for the same coolant and the same operating conditions. For this, we present a comparison between the dynamic behavior and the air circulating in a solar collector equipped with zigzag baffles (case1), and a solar collector equipped with plane baffles (case 2). Other authors studied the effect of the size and orientation of the baffles on heat transfer enhancement inside a tube heat exchanger, taking the example of the work of Nasiruddin and Siddiqui [10] who studied three different orientations of the baffles. The first case considered a vertical baffle, the second one a baffle inclined toward the downstream side and the third one a baffle inclined toward the upstream side. Similarly, Prashanta *et al.* [11] carried out an experimental study on heat losses by friction and also on the behavior of turbulent flow with heat transfer inside a rectangular channel

with flux heating of the upper surface. They used two inclined, solid and perforated baffles with different sizes, positions, and orientations.

2 Mathematical formulation

Solar collector equipped with baffles has been considered. We study two different geometries for the same coolant and the same operating conditions. For this, we present a comparison between the dynamic behavior and the air circulating in a solar collector equipped with zigzag (case 1), and plane (case 2) baffles.

2.1 A geometry of the problem

The geometry of the problem is presented in Fig. 1. It is a rectangular duct, equipped with two zigzag-shaped baffles, traversed by a stationary

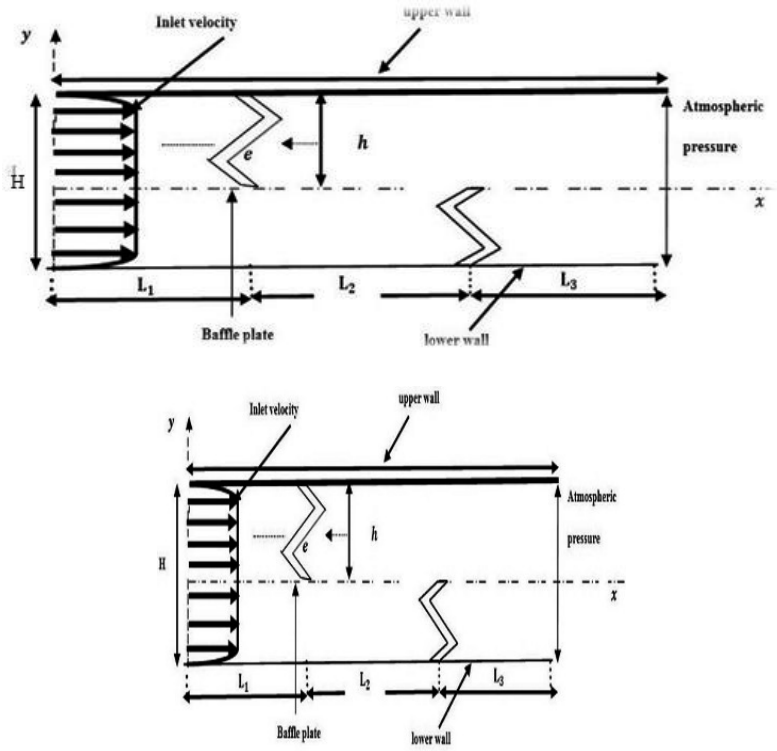

Figure 1: Representative diagram of the problem: zigzag baffles (case 1), plane baffles (case 2).

turbulent air flow, which satisfies the following hypotheses:

- physical properties of air are assumed to be constant,
- velocity profile is uniform at the channel entrance,
- flow is considered as steady,
- effects of induced buoyancy are supposed to be negligible.

Based on the experimental work of Demartini *et al.* [13], it was decided to carry out an air flow test under the following conditions:

- channel length $L = 0.554$ m,
- channel height $H = 2h = 0.143$ m,
- fin height $e = 0.08$ m,
- distance between the channel inlet and the first wing L_1=0.223 m,
- spacing between two wings L_2=0.152 m,
- distance between the second wing and the channel outlet L_3=0.179 m,
- hydraulic diameter $D_h = 0.14$ m,
- Reynolds number Re = 5000,
- inlet velocity $U_{in} = 0.45$ m/s.

2.2 Governing equations

The flow equations used to simulate the incompressible and steady flow of air in the given area of computation are given by:
conservation of mass

$$\frac{\partial(\rho u)}{\partial x} + \frac{\partial(\rho \nu)}{\partial y} = 0\,, \tag{1}$$

conservation of momentum

$$\begin{aligned}
\rho u\frac{\partial u}{\partial x} + \rho\nu\frac{\partial u}{\partial y} &= -\frac{\partial P}{\partial X} + \frac{\partial}{\partial x}\left[(\mu+\mu_t)\left(2\frac{\partial u}{\partial x}\right)\right] \frac{\partial}{\partial y}\left[(\mu+\mu_t)\left(\frac{\partial u}{\partial y} + \frac{\partial \nu}{\partial x}\right)\right],\\
\rho u\frac{\partial \nu}{\partial x} + \rho\nu\frac{\partial \nu}{\partial y} &= -\frac{\partial P}{\partial X} + \frac{\partial}{\partial x}\left[(\mu+\mu_t)\left(2\frac{\partial \nu}{\partial x}\right)\right] \frac{\partial}{\partial y}\left[(\mu+\mu_t)\left(\frac{\partial u}{\partial y} + \frac{\partial \nu}{\partial x}\right)\right],
\end{aligned} \tag{2}$$

conservation of energy for the fluid

$$\rho u\frac{\partial T}{\partial x} + \rho\nu\frac{\partial T}{\partial y} = \frac{\partial}{\partial x}\left[\left(\frac{\mu}{\mathrm{Pr}} + \frac{\mu_t}{\sigma_T}\right)\frac{\partial T}{\partial x}\right] + \frac{\partial}{\partial y}\left[\left(\frac{\mu}{\mathrm{Pr}} + \frac{\mu_t}{\sigma_T}\right)\frac{\partial T}{\partial y}\right], \tag{3}$$

conservation of energy in the wall

$$\left(\frac{\partial^2 T}{\partial x^2} + \frac{\partial^2 T}{\partial y^2}\right) = 0\,. \tag{4}$$

2.3 Equations of turbulence

A comparative study was conducted on four models of turbulence, namely the Spalart Allmaras model [12], the k-ε model, the k-ω model, k-ω shear stress transport turbulence (SST) model and the Reynolds stress model, which were evaluated through the resolution of the Navier–Stokes equations. It has been found that the k-ω SST model is the most accurate in predicting flow changes in the presence of baffles. The chosen turbulence model allowed to calculate the rapidly changing two-dimensional flux and also to anticipate interactions with the wall. Another advantage of the selected turbulence model is that the model equations behave suitably in the regions both in the vicinity of the wall and far away from it as well.

The k-ω model is defined by two transport equations, one for the turbulent kinetic energy k and the other for the specific dissipation rate ω:

$$\frac{\partial}{\partial t}(\rho\omega) + \frac{\partial}{\partial x_i}(\rho\omega u_i) = \frac{\partial}{\partial x_j}\left(\Gamma_\omega \frac{\partial \omega}{\partial x_j}\right) + G_\omega - Y_\omega + D_\omega + S_\omega\,, \tag{5}$$

where:

$$G_k = -\rho\overline{u_i' u_j'}\frac{\delta u_j}{\delta x_i}\,, \qquad G_\omega = \alpha\frac{\omega}{k}G_k\,, \tag{6}$$

$$\Gamma_k = \mu + \frac{\mu_t}{\sigma_k}\,, \qquad \Gamma_\omega = \mu + \frac{\mu_t}{\sigma_\omega}\,. \tag{7}$$

Here the overbar denotes an average value.

The Reynolds number, for the rectangular duct, can then be defined as

$$\mathrm{Re} = \frac{D_h U_{in}\rho}{\mu}\,. \tag{8}$$

The friction coefficient and the pressure drop in different sections of the pipe may be calculated using the following relationships:

$$f = \frac{2\tau_\omega}{\rho U^2}\,, \tag{9}$$

$$\Delta P = \frac{f L \rho U^2}{2h}\,. \tag{10}$$

2.4 Boundary conditions

(I) A uniform velocity was applied, as a boundary condition, and the pressure was set to zero at the entrance of the computational domain.

(II) Two horizontal walls of the computational domain were both held at the constant temperature of 375 K. This constitutes a thermal boundary condition.

(III) Temperature of the fluid used was set at 300 K at the inlet of the canal.

2.5 Numerical resolution

The finite volume method has been applied for the numerical resolution of the system of equations described above. The SIMPLEC (semi-implicit method for pressure linked equations-consistent) algorithm proposed by Patankar [14] was used for pressure and velocity correction. The QUICK (quadratic upstream interpolation for convective kinematics) scheme is used for the discretization of the terms of convection. A structured and non-uniform mesh was used, depending on the case under study, with a refined mesh in the areas containing the baffles and near the walls, in order to capture the strong gradients of temperature and velocity. Several tests were performed in order to ensure that the results do not depend on the refining of the mesh. The iterative procedure was continued until the residuals for all computing cells were less than 10^{-8} for all quantities analyzed.

3 Results and interpretation

3.1 Validation of the model

To validate our numerical modeling, the results obtained were compared with those reported in the work of Demartini *et al.* [13] who experimentally studied the dynamic behavior of an airflow inside a rectangular duct equipped with plane baffles, with the Reynolds number equal to 5000.

Comparing the results obtained for the axial velocity with the experimental ones of Demartini *et al.* [13], as presented in Fig. 2, and for the axial position $x = 0$ m, one can note that the two series of results are in good agreement.

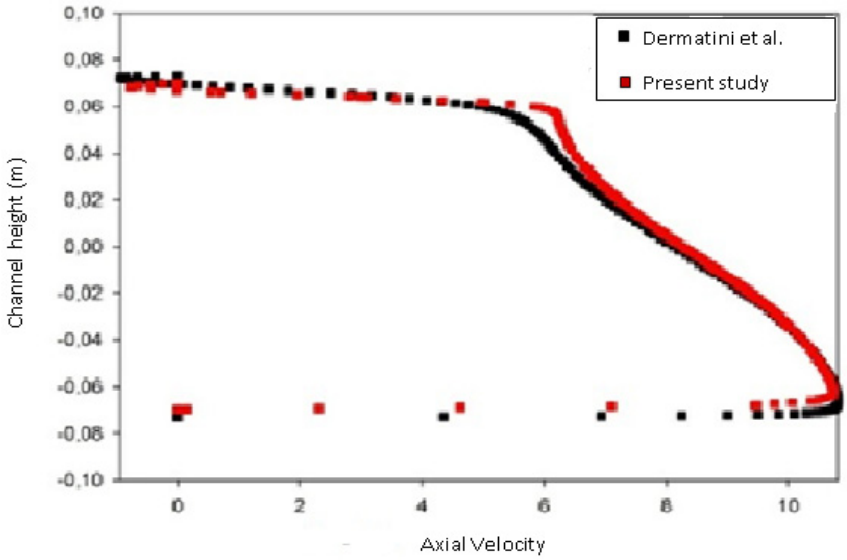

Figure 2: Validation of numerical simulation for the position $x = 0.159$ m with the experimental results of Demartini *et al.* [13].

3.2 Hydrodynamic aspect

Figure 3 shows the velocity field for both treated cases: zigzag baffles (a) and plane baffles (b). It is clear that the velocity values are very low near the two baffles, especially in the downstream regions, because of the presence of the recirculation zones. We also note the increase in velocity in the space between the top of each baffle and walls of the channel. This increase is

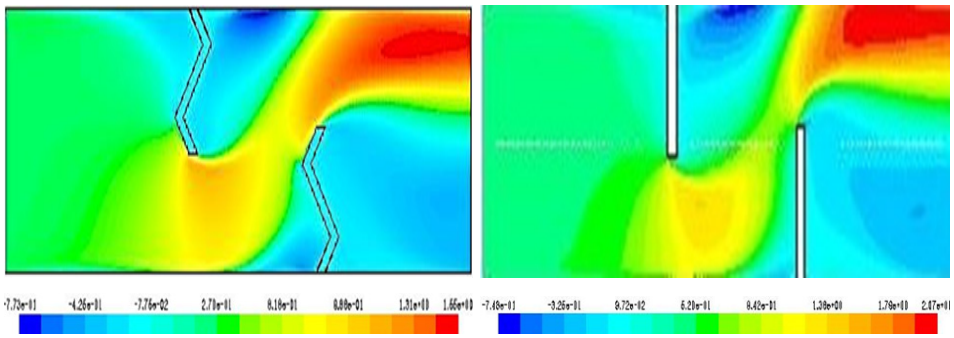

(a) (b)

Figure 3: Contour of the axial velocity.

generated firstly by the presence of obstacles, as well as by the presence of a recirculating fluid which then results in an abrupt change in the direction of flow. The average axial velocity profiles for the different types of baffles studied, namely a baffle in zigzag or plane baffle form are given in Figs. 4–10, respectively, for different sections: $x = 0.159$, 0.189, 0.255, 0.285, 0.315, 0.345, 0.525 m.

Figures 4 and 5 show the velocity profiles upstream of the first baffle in the two cases treated for the two sections at $x = 0.159$ m and $x = 0.189$ m. It has been noted that the presence of the first baffle which is in the upper half of the channel induces a sharp decrease in the speed as the use of one of the two forms of baffle (plane or zigzag) does not affect the dynamic behavior of the air upstream of the first baffle.

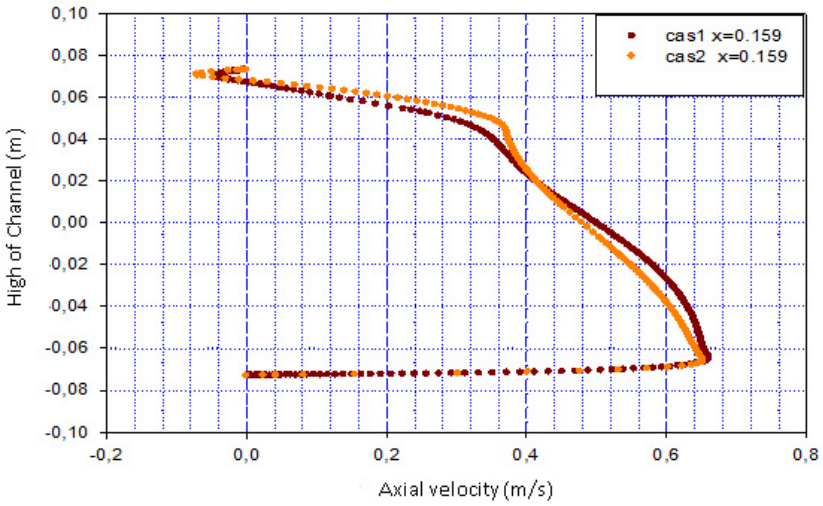

Figure 4: Axial velocity profiles upstream of the first baffle for both treated baffle shapes, $x = 0.159$ m.

In the intermediate zone, the flow is characterized by very high velocities at the lowest part of the channel. In the upper part of the channel, the negative velocities indicate presence of the recirculation of the flow behind the first baffle. What has been noticed too, the flow in the presence of baffles of zigzag shapes is accelerating more and more from left to right by increasing the size of the recirculation zone Figs. 6 and 7.

Figures 8 and 9 show that the flow approaching the second baffle, its velocity is increased at the bottom of the channel. The maximum values of

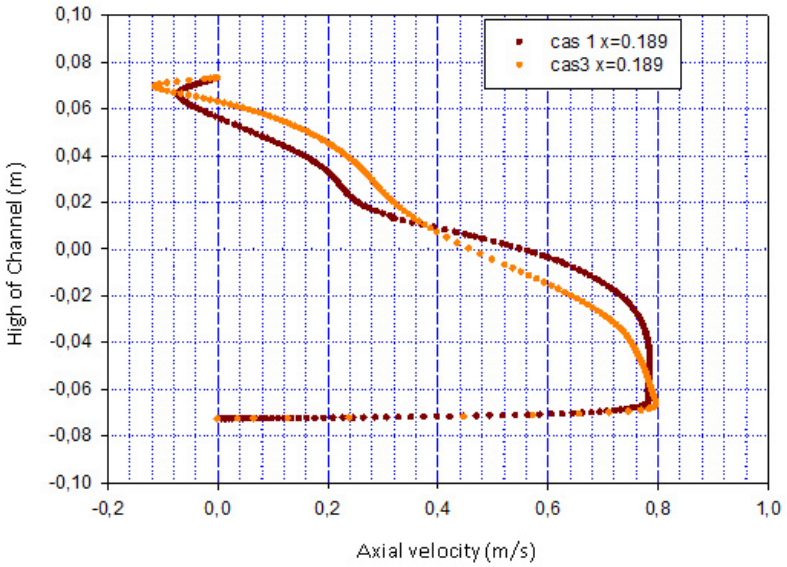

Figure 5: Axial velocity profiles upstream of the first baffle for both forms of treated baffles, $x = 0.189$ m.

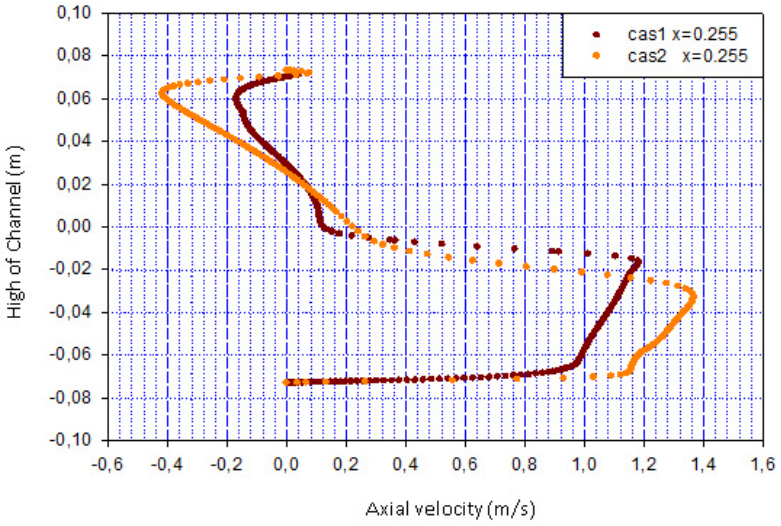

Figure 6: Velocity profiles between the first and second baffle, $x = 0.255$ m.

the axial velocity in both cases reached about 2.05 m/s, which is 4.5 times higher than the input velocity (0.45 m/s). We find that our case provides a higher velocity than that of Demartini *et al.* [13].

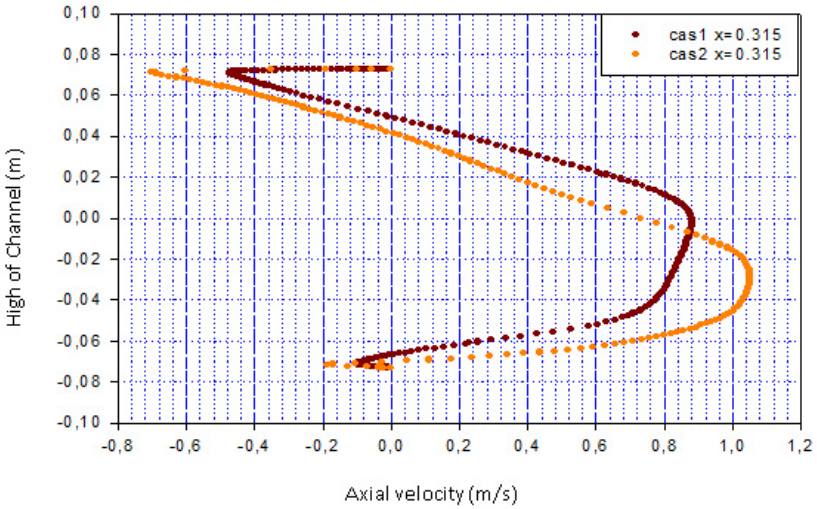

Figure 7: Axial velocity profiles upstream of the second baffle, $x = 0.315$ m.

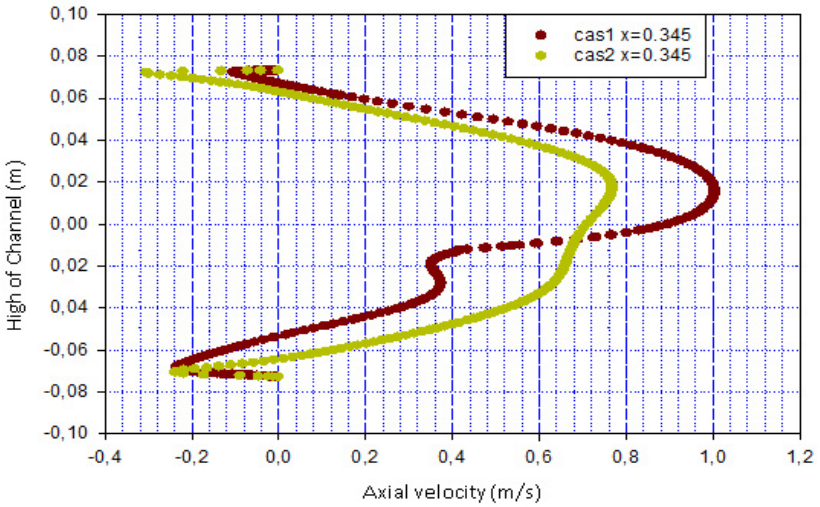

Figure 8: Profiles of the axial velocity upstream of the baffle, $x = 0.345$ m.

The coefficient of friction induces an increase in the pressure drop, so we find that the plane shape in the baffles induces high losses (Fig. 10). From the point of view of the chicane, it is interesting to study the influence of Reynolds numbers on the variation of the coefficient of friction. Fig-

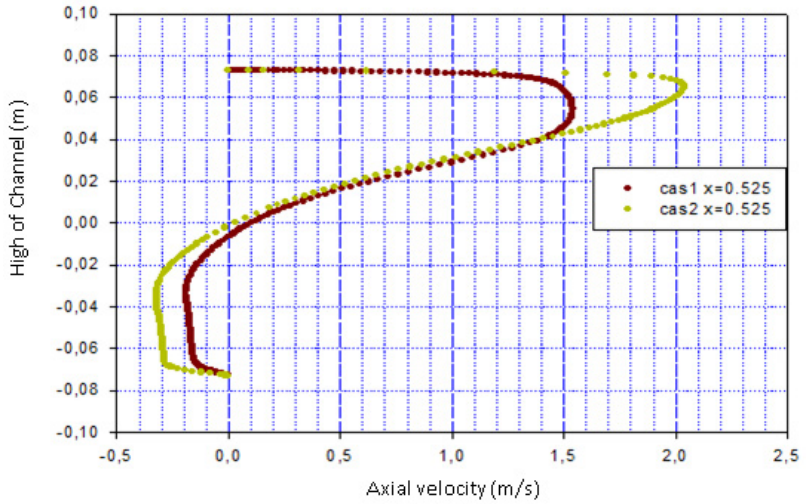

Figure 9: Axial velocity profiles near the channel exit, $x = 0.525$ m.

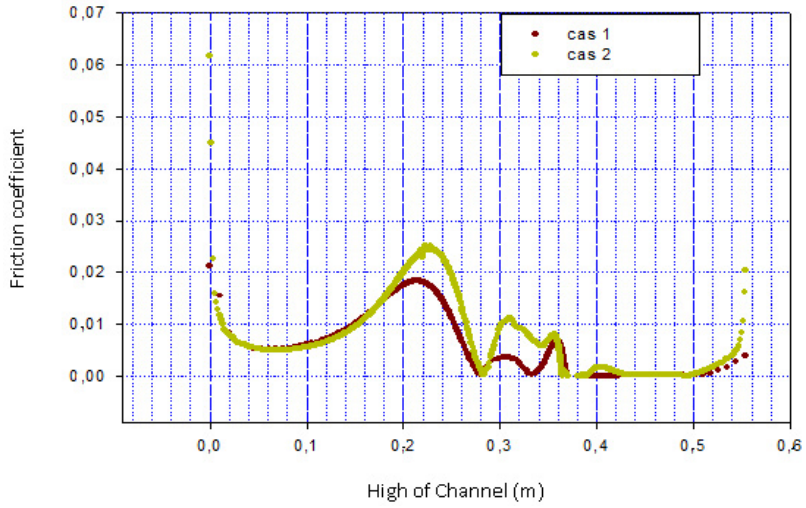

Figure 10: Variation of the local coefficient of friction along the lower wall of the channel.

ures 11 and 12 show this dependency. It is presented for both cases and for a Reynolds ranging from 5000 to 25 000. The increase of the latter induces a friction increase and therefore the pressure drop and more significantly after a Reynolds value equal to 7.5812×10^{-3} for the top wall.

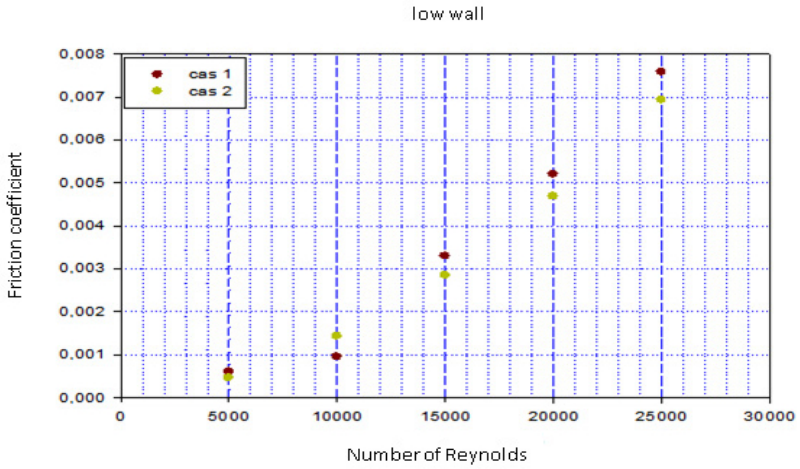

Figure 11: Variation in mean friction coefficient along the lower wall of the channel versus Reynolds number.

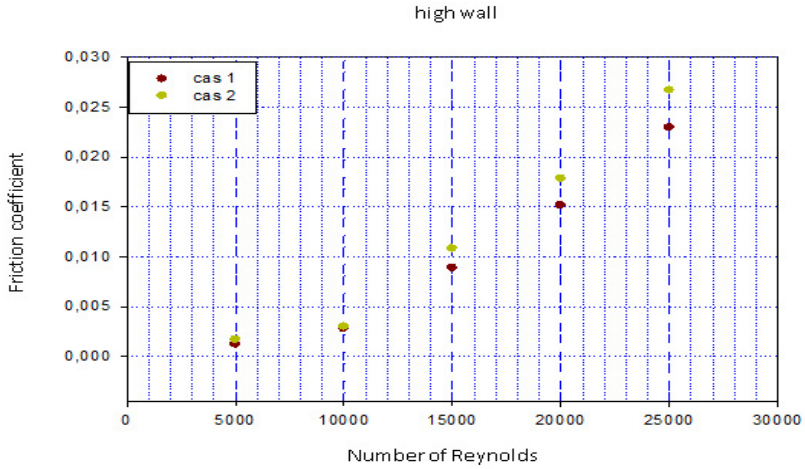

Figure 12: Variations in mean friction coefficient along the higher wall of the channel versus Reynolds number.

4 Conclusion

To improve mixing and therefore, heat transfer the effects of the baffle shape (plane and zigzag) on the dynamic behavior of the flow have been studied in detail. The numerical results obtained are compared with experimental results from the literature to analyze the thermal behavior of

a turbulent air flow using the model k–ω achievable in a rectangular channel provided with baffles of different geometries. The profiles and the axial velocity distribution show a relatively intense recirculation zone above the faces of each baffle moving downstream. The use of zigzag– shaped baffles ensures a considerable increase in velocity in comparison to the flat– shaped baffles.

Received 3 March 2020

References

[1] Promvonge P., Kwankaomeng S.: *Periodic laminar flow and heat transfer in a channel with 45° staggered V– baffles*. Int. Commun. Heat Mass **37**(2010), 7, 841–849.

[2] Abene A. et al: *Study of a solar air flat plate collector: use of obstacles and application for the drying of grape*. J. Food Eng. **65**(2004), 1, 15–22.

[3] Sripattanapipat S., Promvonge P.: *Numerical analysis of laminar heat transfer in a channel with diamond-shaped baffles*. Int. Commun. Heat Mass **36**(2009), 1, 32–38.

[4] Ahmed-Zaïd, Moulla A., Hantala M.S., Desmons J.Y.: *Amélioration des Performances des Capteurs Solaires Plans à Air:Application au Séchage de l'Oignon*. Jaune et du Hareng, Revue des Energies Renouvelable **4**(2001) 2, 69–78.

[5] Aoues K., Moummi N., Moummi A., Zellouf M., Labed A., E. Achouri: *Etude de l'influence des rugosité – artificielles sur les performances thermiques des capteurs solaires plans à air*. Revue des Energies Renouvelables **11**(2008), 2, p 219–227.

[6] Yuna Z.X., Wang Q.W.: *Experimental study of enhanced heat transfer in ducts with periodic rectangular fins along the main flow direction*. In: Proc. Heat Transfer Conf. 23–28 August, Kyongju, Korea **5**(1998), 327– 332.

[7] Acharya S., Myrum T.: *Developing and periodically developed flow, temperature and heat transfer in a ribbed duct*. Int. J. Heat Mass Tran. **40**(1997), 461–479.

[8] Roetzel W., Deiving W.Lee.: *Effect of baffle/channel leakage flow on heat transfer in shell– and– tube heat exchanger*. Exp. Therm. Fluid Sci. **8**(1994), 1, 10–20.

[9] Molki M., Mostoufizadeh A.R: *Turbulent heat transfers in rectangular ducts with repeated– baffle blockages*. Int. J. Heat Mass Tran. **32**(1989), 8, 1491–1499.

[10] Nasiruddin M.H., Siddiqui K.: *Heat transfer augmentation in a heat ex-changer tube using a baffle*. Int. J. Heat Fluid Fl. **28**(2007), 2, 318–328.

[11] Cui H., Horiuchi K., Dutta P., Ivory C.F.: *Multistage isoelectric focusing in a polymeric microfluidic*. Anal. Chem. **77**(1998), 24, 7878–7886.

[12] Spalart P.R., Allmaras S.R.: *A one– equation turbulence model for aerodynamic flows*. AIAA (1992), 92–0439.

[13] Dermatini L.C., Vielmo H.A., Moller S.V.: *Numeric and experimental analysis ofthe turbulent flow through a channel with baffle plates*. J. Braz. Soc. Mech, Sci. vvd. Sci. **26**(2004), 2.

[14] Patankar S.V.: *Numerical Heat Transfer and Fluid Flow*. Hemisphere, Washington, DC. 1980.